



Donepezil attenuates progression of cardiovascular remodeling and improves prognosis in spontaneously hypertensive rats with chronic myocardial infarction

Meihua Li¹ · Can Zheng^{1,2} · Toru Kawada¹ · Kazunori Uemura³ · Shohei Yokota¹ · Hiroki Matsushita¹ · Keita Saku^{1,3}

Received: 6 November 2023 / Revised: 25 January 2024 / Accepted: 18 February 2024 / Published online: 14 March 2024
© The Author(s), under exclusive licence to The Japanese Society of Hypertension 2024

Abstract

The acetylcholinesterase inhibitor donepezil restores autonomic balance, reduces inflammation, and improves long-term survival in rats with chronic heart failure (CHF) following myocardial infarction (MI). As arterial hypertension is associated with a significant risk of cardiovascular death, we investigated the effectiveness of donepezil in treating CHF in spontaneously hypertensive rats (SHR). CHF was induced in SHR by inducing permanent MI. After 2 weeks, the surviving SHR were randomly assigned to sham-operated (SO), untreated (UT), or oral donepezil-treated (DT, 5 mg/kg/day) groups, and various vitals and parameters were monitored. After 7 weeks of treatment, heart rate and arterial hypertension reduced significantly in DT rats than in UT rats. Donepezil treatment improved 50-day survival (41% to 80%, $P = 0.004$); suppressed progression of cardiac hypertrophy, cardiac dysfunction (cardiac index: 133 ± 5 vs. 112 ± 5 ml/min/kg, $P < 0.05$; left ventricular end-diastolic pressure: 12 ± 3 vs. 22 ± 2 mmHg, $P < 0.05$; left ventricular $+dp/dt_{\max}$: 5348 ± 338 vs. 4267 ± 114 mmHg/s, $P < 0.05$), systemic inflammation, and coronary artery remodeling (wall thickness: 26.3 ± 1.4 vs. 34.7 ± 0.7 μm , $P < 0.01$; media-to-lumen ratio: 3.70 ± 0.73 vs. 8.59 ± 0.84 , $P < 0.001$); increased capillary density; and decreased plasma catecholamine, B-type natriuretic peptide, arginine vasopressin, and angiotensin II levels. Donepezil treatment attenuated cardiac and coronary artery remodeling, mitigated cardiac dysfunction, and significantly improved the prognosis of SHR with CHF.

Keywords Donepezil · Hypertension · Myocardial infarction · Cardiovascular remodeling · Chronic heart failure

Introduction

The prevalence of chronic heart failure (CHF) continues to increase rapidly worldwide, and mortality and morbidity rates among patients with CHF remain unacceptably high despite the practice of guideline-directed medical therapy [1–3]. In recent decades, significant progress has been achieved in treating CHF by targeting autonomic dysfunction associated

with persistent compensatory mechanisms, which are key determinants of long-term morbidity and mortality [4–6]. CHF pathophysiology involves sympathetic over-activity and parasympathetic withdrawal [7, 8]. The detrimental health effects of excessive neurohumoral activation have led to the use of beta-blockers, angiotensin-converting enzyme inhibitors (ACEIs), angiotensin II receptor blockers (ARBs), and an angiotensin receptor-neprilysin inhibitor (ARNI) in patients with CHF, resulting in improved survival rates [9].

Decreased parasympathetic activity is an independent risk factor following acute myocardial infarction (MI) [10, 11]. We demonstrated that parasympathetic activation via electrical vagal nerve stimulation significantly improved long-term survival in rats with CHF following MI [12]. Although the vagal nerve structure and function potentially differ between species, vagal nerve stimulation has also been investigated in clinical trials [13–15]. Additionally, we propose a novel pharmacotherapy for modulating parasympathetic function using donepezil, which is a centrally-

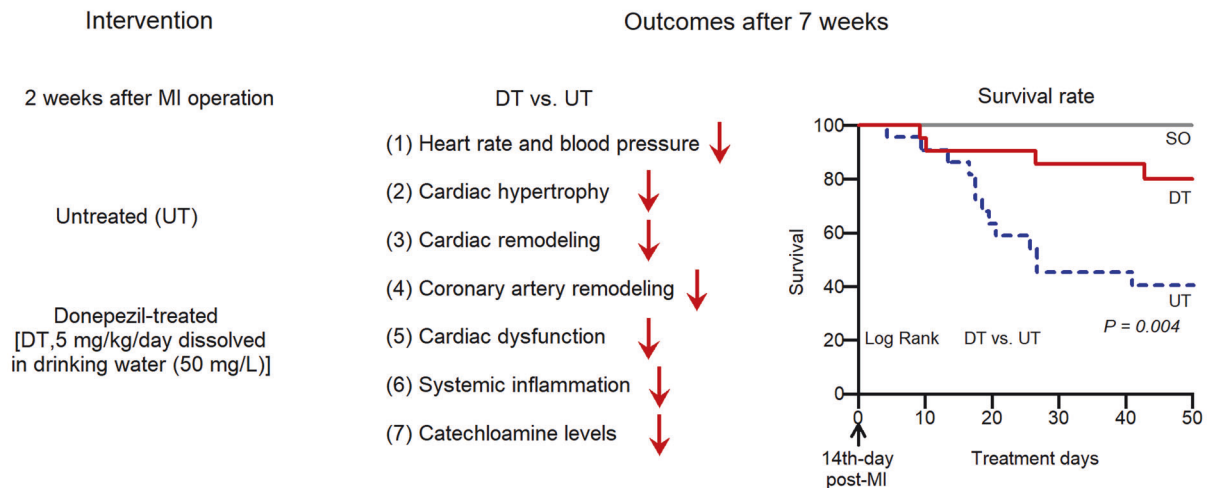
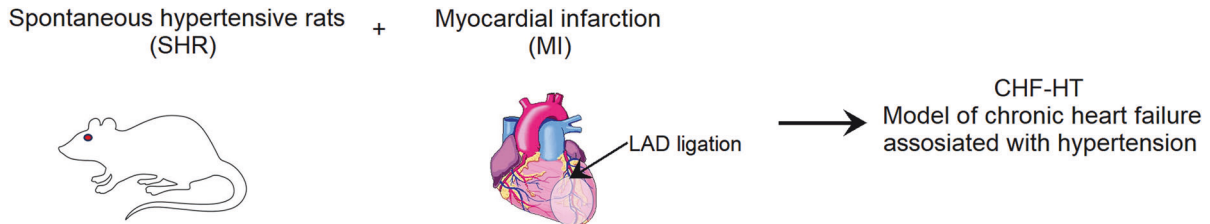
✉ Meihua Li
limeihua@ncvc.go.jp

¹ Department of Cardiovascular Dynamics, National Cerebral and Cardiovascular Center, Osaka 564-8565, Japan

² New Business Development Group, Business Planning Department, Sanyo Chemical Industries, LTD, Kyoto, Japan

³ Bio Digital Twin Center, National Cerebral and Cardiovascular Center, Osaka 564-8565, Japan

Graphical Abstract



Conclusion: Donepezil treatment effectively prevented cardiovascular remodeling and improved survival in CHF-HT rats.

acting acetylcholinesterase (AChE) inhibitor. Donepezil effectively prevented the progression of cardiac remodeling and improved the long-term prognosis of rats with CHF following extensive MI in both monotherapy and combination therapy with losartan [16, 17]. Donepezil is commonly prescribed for Alzheimer's disease (AD) and vascular dementia to increase central acetylcholine (ACh) levels. Donepezil administration exerted cardioprotective effects by supporting the vagal tone through central mechanisms [18] and by exhibiting anti-inflammatory effects [19].

In our previous studies investigating the beneficial effect of donepezil, we induced CHF by coronary artery ligation in normotensive Sprague–Dawley (SD) rats [16, 17]. The model differed from clinical CHF in that the SD rats had normal heart and vasculature before the induction of MI. Meanwhile, hypertension and ischemic heart disease represent important etiologic factors leading to CHF [20]. Hypertension results in hypertensive vascular remodeling and increased total peripheral resistance [21]. Hypertensive hearts frequently result in MI and then develop CHF. However, the effectiveness of donepezil in treating CHF associated with hypertension (CHF-HT) remains unknown. Therefore, we examined the effects of donepezil on spontaneously hypertensive rats (SHR) with CHF following MI

to test the hypothesis that donepezil can be used to treat CHF-HT.

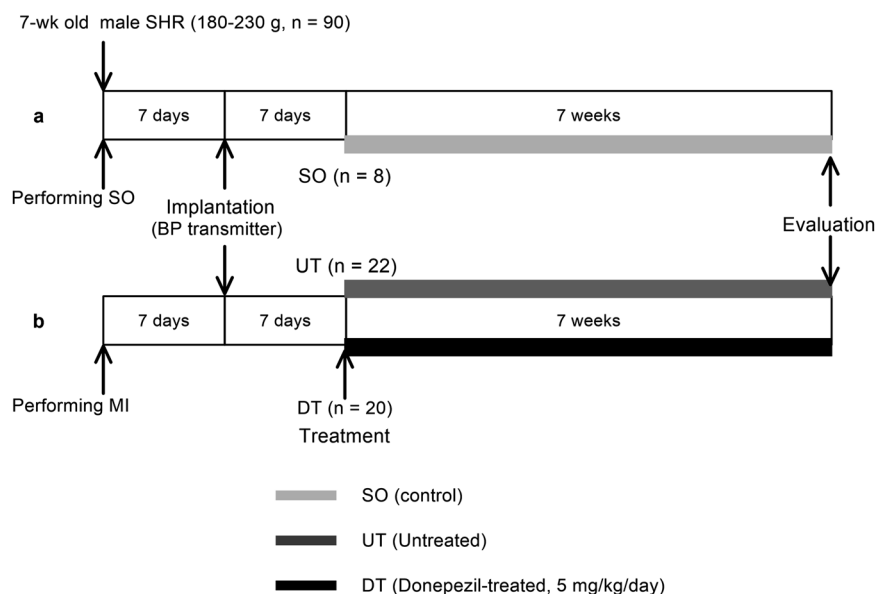
Methods

A previous study has demonstrated that SHR has cardiac hypertrophy compared with its normotensive counterpart, Wistar–Kyoto (WKY) rats, and post-MI SHR better reproduces CHF symptoms compared with post-MI WKY rats [22]. In this study, 90 male SHR (180–230 g; Japan SLC) were used. The rats were cared for in strict accordance with the Guiding Principles for the Care and Use of Animals in the Field of Physiological Sciences, approved by the Physiological Society of Japan. The Animal Subjects Committee of the National Cerebral and Cardiovascular Center reviewed and approved all experimental protocols (15004 and 16002). The animals were housed individually with free access to food and water and maintained on a 12-h light/dark cycle.

Surgical preparation and experimental protocol

The experimental protocol is illustrated in Fig. 1. At 7 weeks of age, CHF was induced in the SHR as a result of

Fig. 1 Experimental event and protocol. **a** Sham operation (SO, $n = 8$) in spontaneously hypertensive rats (SHR). **b** Inducing permanent myocardial infarction (MI) in the SHR. The surviving animals were randomly assigned to the untreated (UT, $n = 22$) or donepezil-treated (DT, $n = 20$) groups for cardiovascular remodeling and prognosis studies



permanent MI, as previously described [12, 16]. One week later, radio telemetry transmitters (TA11PA-C40, DSI, St. Paul, MN, USA) were implanted in the surviving rats to measure the blood pressure (BP) and heart rate (HR) under conscious state. Two weeks after the induction of MI, the SHR were randomly divided into untreated (UT) and donepezil-treated [DT, 5 mg/kg/day dissolved in drinking water (50 mg/L)] groups. SHR in the sham operation (SO) group underwent thoracotomy without coronary artery ligation. During all the experiments, the animals were anesthetized with halothane (3% at induction, 1.2% during surgery, and 0.6% during data recording) and ventilated through an endotracheal cannula. The body temperature was maintained at 37 °C.

Hemodynamic measurements and cardiac remodeling assessment

The 50-day survival was observed from 2 weeks after MI. Then, we measured the hemodynamics of the surviving rats under anesthesia. Left ventricular (LV) and arterial pressures were measured using a 2-Fr catheter tip micro-manometer (SPC-320; Millar Inc., Houston, TX, USA), and aortic flow was measured using an ultrasonic flow probe (T206 flow probes #2.5 SB; Transonic Systems Inc., NY, USA). Effective arterial elastance (E_a) was calculated based on the formula $E_a = \text{LV end-systolic pressure (LVESP)} / \text{stroke volume}$, where the stroke volume = cardiac output/HR. Right atrial pressure (RAP) was measured using a fluid-filled pressure transducer. All signals were digitized at a rate of 500 Hz for 1 min. Once the hemodynamic measurements were made, blood samples were collected from the carotid artery and centrifuged at 4 °C. The plasma

samples were then separated and stored at -80 °C until needed for further assays. Finally, the experimental animals were euthanized using an overdose of intravenous sodium pentobarbital. The heart was rapidly excised and weighed after the blood was rinsed off. It was sliced with a stainless-steel slicer, and paraffin-embedded for determination of infarct size and histological examination.

Plasma neurohumoral and cytokine measurement

Plasma catecholamine levels were measured using high-performance liquid chromatography with electrochemical detection after alumina adsorption. Plasma levels of B-type natriuretic peptide (BNP), arginine vasopressin (AVP), and angiotensin II (Ang II) were determined using ELISA (BNP-32 Enzyme Immunoassay Kit, Peninsula Lab, CA, USA; arg8 -Vasopressin Enzyme Immunoassay Kit, Assay Designs, MI, USA; and angiotensin II enzyme immunoassay kit, SPI Bio, UK). Tumor necrosis factor (TNF)- α and C-reactive protein (CRP) were measured using ELISA (Rat TNF- α immunoassay kit, TECHNE Corporation, MN, USA; Rat High-Sensitive CRP ELISA kit, Kamiya Biomedical Company, WA, USA).

Histological assessment of infarct size, myocardial fibrosis, perivascular fibrosis, and coronary artery

The heart sections (4- μm thickness) were deparaffinized and stained with either Masson's trichrome to detect myocardial fibrosis or Elastic van Gieson's (EVG) to stain elastic fibers. Histological images were obtained and analyzed using a microscope (BZ-9000; Keyence, Osaka, Japan) equipped with image analysis software. The infarct size was

calculated based on the endocardial lengths of the infarcted regions relative to the LV endocardial circumferences. The extent of myocardial fibrosis was evaluated at 20× magnification in eight fields in the non-infarcted area. Perivascular fibrosis and the coronary artery were analyzed by examining the vessels that had inner diameters of 50–100 µm in the non-infarcted area at 40× magnification.

Immunohistological assessment of myocardial capillary vessels and coronary artery

Immunohistochemical triple staining for von Willebrand factor (vWF), smooth muscle actin (SMA), and 4',6-diamidino-2-phenylindole dihydrochloride (DAPI) was performed on deparaffinized heart sections. The sections were incubated overnight with rabbit anti-human vWF polyclonal antibody (DakoCytomation, Denmark) and mouse anti-human SMA monoclonal antibody (DakoCytomation, Denmark) at 4 °C. Then, they were incubated with Alexa 633-conjugated goat anti-rabbit IgG and Alexa 488-conjugated goat anti-mouse IgG (Invitrogen, OR, USA), and the capillary vessels and coronary arteries were analyzed. The fluorescence emitted by Alexa 633, Alexa 488, and DAPI (Alexa 350) was observed using a laser scanning microscope (BZ-9000; Keyence, Osaka, Japan). The number of capillary vessels in the peri-infarcted area and non-infarcted septa were counted using a laser scanning microscope at 20× magnification in six fields. The coronary arteries in the non-infarcted area were analyzed at 40× magnification. The data obtained from the high-power fields were averaged, and the number of capillary vessels and wall thickness of the coronary arteries in each heart were recorded.

Survival rate

The 50-day survival rates in the three groups (SO, $n = 8$; UT, $n = 22$; DT, $n = 20$) were analyzed to examine the outcomes of the donepezil therapy. The rats were inspected daily, and a gross postmortem examination was conducted on the dead rats. We classified the cause of death as heart failure if we observed edema, extreme weight loss accompanied by panting over 24 h prior to death, or pleural effusion. Otherwise, we classified the cause of death as sudden cardiac death due to arrhythmia.

Statistical analysis

All statistical analyses were performed using GraphPad StatMate Prism 7. All data are expressed as the mean ± standard error of the mean (SEM). The differences in the long-term recorded HR and mean BP (MBP) before and during treatment in each group were examined using a one-

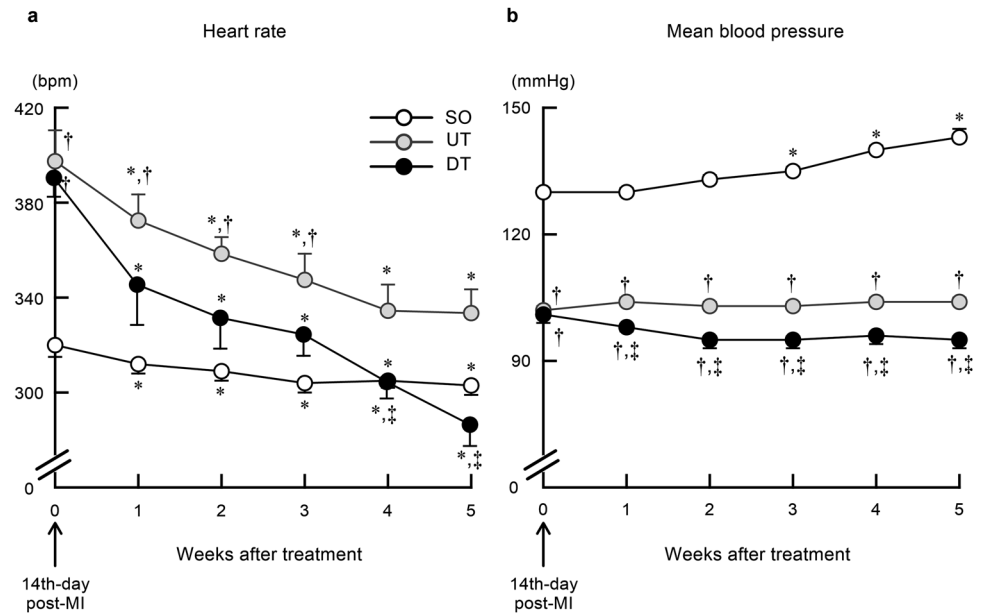
way analysis of variance (ANOVA) for repeated measures, followed by Dunnett's test. Differences among the three groups (SO, UT, and DT) were examined using one-way ANOVA, followed by Tukey's multiple comparison tests. For hemodynamic measurements under anesthesia and remodeling data, differences among the three groups were tested using one-way ANOVA followed by Tukey's multiple comparison tests. For cardiac fibrosis and perivascular fibrosis, differences among the three groups were tested using nonparametric Kruskal–Wallis tests, followed by Dunn's tests. The neurohumoral and biochemical data were also first analyzed using nonparametric Kruskal–Wallis tests, and the overall differences were not detected among the three groups. However, the number of samples in the SO group was 5 due to blood sampling failure, which might have reduced the statistical power to detect the differences among the three groups. Accordingly, we performed a subanalysis only between the UT and DT groups using the nonparametric Mann–Whitney U-tests, with the limitation in mind that the P values should be higher when they are corrected for multiple comparisons. For coronary artery remodeling data, we did not investigate the data in the SO group, and the comparison was made between the UT and DT groups using the nonparametric Mann–Whitney U-tests. Survival data are presented as Kaplan–Meier curves, and 50-day survival was analyzed using a log-rank test. In all statistical analyses, $P < 0.05$ was considered statistically significant.

Results

Telemetric hemodynamic measurements in the conscious state

Obtaining the continuous 5-week hemodynamic recording was not successful for all rats because of difficulties in measuring telemetric arterial pressure. The arterial pressure waveform in some rats was strange, yet the HR was properly detected for the analysis. Therefore, the numbers of rats analyzed for HR data were 6, 7, and 8 in the SO, UT, and DT groups, respectively; those analyzed for MBP data were 6, 5, and 5 in the SO, UT, and DT groups, respectively. Compared with the SO group, post-MI SHR in the UT and DT groups presented a higher HR (> 67 bpm) and lower MBP (< -28 mmHg) on day 14 post-MI before the commencement of treatment (Fig. 2). Post-MI SHR showed a decreasing trend for HR for the following 5 weeks. A significant reduction in HR was observed from week 1 of treatment in both UT and DT groups. The difference in HR between the DT and UT groups reached approximately 50 bpm on week 5 of treatment (287 ± 9 vs. 334 ± 10 bpm, $P < 0.01$) (Fig. 2a). The DT group exhibited slightly but

Fig. 2 Hemodynamic changes recorded using a telemetry system. **a** Weekly averaged heart rate (HR) and **b** mean blood pressure (MBP). Each point represents the 1-week averaged data in each group [HR (SO, $n = 6$; UT, $n = 7$; DT, $n = 8$); MBP (SO, $n = 6$; UT, $n = 5$; DT, $n = 5$)]. Values are presented as mean \pm SEM. * $P < 0.05$ vs. pretreatment values (week 0) of each group by one-way ANOVA with repeated measures and post-hoc Dunnett's test. Differences among the three groups (SO, UT, and DT) were examined with one-way ANOVA, followed by Tukey's multiple comparison tests. † $P < 0.05$ vs. SO and ‡ $P < 0.05$ vs. UT



significantly lower MBP than did the UT group from week 1 of treatment (98 ± 1 vs. 104 ± 1 mmHg, $P < 0.05$) (Fig. 2b).

The hemodynamic measurement under anesthesia and cardiac remodeling

The hemodynamic parameters of the surviving rats after 7 weeks of treatment were measured under anesthesia (Table 1). Compared with the SO group, post-MI SHR in the UT and DT groups had lower body weight (BW) and higher heart weight (HW). The post-MI SHR also exhibited lower values for MBP, LVESP, cardiac index (CI), HR, positive and negative maximum dp/dt of LV pressure ($LV \pm dp/dt_{max}$), E_a , and systemic vascular resistance index (SVRI), whereas they exhibited higher values for LV end-diastolic pressure (LVEDP) and RAP. Compared with the UT group, the DT group had significantly higher MBP, CI, and $LV \pm dp/dt_{max}$ values but lower LVEDP, RAP, and E_a values.

Cardiac structure

Although the infarct size did not significantly differ between the UT and DT groups (Table 1), the prevention of cardiac dysfunction in the DT group occurred together with the prevention of cardiac remodeling, as evidenced by the suppression of hypertrophy in HW. Histological analysis of the heart revealed an association between preserved cardiac function and histological changes. Figure 3a–c shows representative images of biventricular sections, myocardial interstitial fibrosis in the non-infarcted area, and perivascular fibrosis in the vessels. Compared with the UT rats, the DT rats presented significantly attenuated myocardial

Table 1 Hemodynamic and cardiac remodeling in SO and post-MI SHR after the 7 weeks of treatment

	SO ($n = 8$)	UT ($n = 9$)	DT ($n = 15$)
BW, g	361 ± 3	$343 \pm 2^*$	$336 \pm 5^{**}$
HW, g/kg	3.46 ± 0.04	$4.09 \pm 0.07^{**}$	$3.83 \pm 0.05^{***\dagger\dagger}$
Infarct size, %	N/A	48 ± 1	50 ± 1
MBP, mmHg	128 ± 3	$89 \pm 4^{**}$	$101 \pm 3^{***\dagger}$
HR, bpm	313 ± 10	$282 \pm 6^*$	$264 \pm 7^{**}$
LVESP, mmHg	160 ± 9	$104 \pm 2^{**}$	$114 \pm 6^{**}$
LVEDP, mmHg	5 ± 3	$22 \pm 2^{**}$	$12 \pm 3^\dagger$
CI, mL/min/kg	139 ± 8	$112 \pm 5^*$	$133 \pm 5^\dagger$
$LV + dp/dt_{max}$, mmHg/s	7212 ± 370	$4267 \pm 114^{**}$	$5348 \pm 338^{***\dagger}$
$LV - dp/dt_{max}$, mmHg/s	6808 ± 296	$3146 \pm 121^{**}$	$4234 \pm 322^{***\dagger}$
RAP, mmHg	3.3 ± 1.1	$7.9 \pm 0.8^*$	$4.1 \pm 1.0^\dagger$
E_a , mmHg/mL	1026 ± 105	780 ± 42	$707 \pm 48^{**}$
SVRI, mmHg \times min \times kg/ mL	0.91 ± 0.05	$0.74 \pm 0.05^*$	$0.71 \pm 0.03^*$

Data are expressed as mean \pm SEM. Differences among the three groups were tested using ANOVA, followed by Tukey's multiple comparison tests. Infarct size was tested using an unpaired t -test

MI myocardial infarction, *SHR* spontaneously hypertensive rats, *BW* body weight, *HW* biventricular weight normalized by BW, *MBP* mean arterial pressure, *HR* heart rate, *LVESP* left ventricular end-systolic pressure, *LVEDP* left ventricular end-diastolic pressure, *CI* cardiac index, $LV + dp/dt_{max}$ positive maximum dp/dt of left ventricular pressure, $LV - dp/dt_{max}$ negative maximum dp/dt of left ventricular pressure, *RAP* right atrial pressure, E_a arterial elastance, *SVRI* systemic vascular resistance index, *SO* sham operation, *UT* untreated, *DT* donepezil-treated, *N/A* not applicable

* $P < 0.05$ and ** $P < 0.01$ vs. SO, † $P < 0.05$ and †† $P < 0.01$ vs. UT

fibrosis (Fig. 3d) and perivascular fibrosis (Fig. 3e), which were similar to the levels observed among the SO rats.

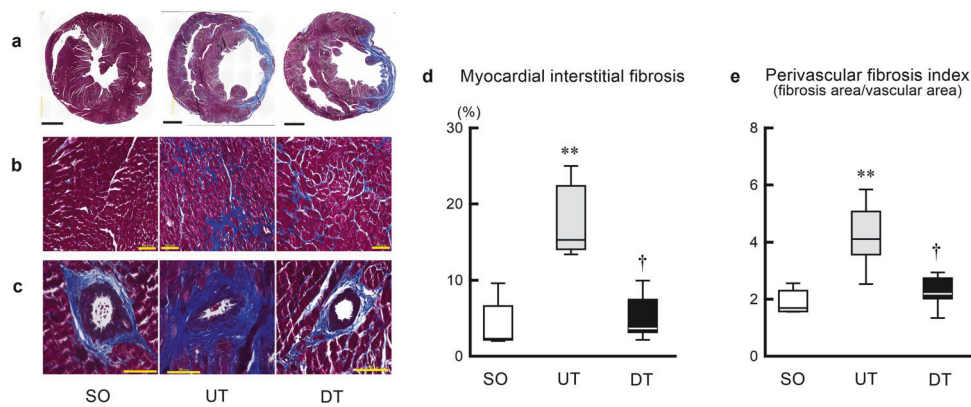


Fig. 3 Masson's trichrome staining on ventricle slices of SO and post-MI SHR in UT and DT groups. **a** Representative biventricular sections without or with MI. Scale bars, 2 mm. **b** Representative image of the myocardial interstitial fibrosis in the non-infarct area. Scale bars, 100 μ m. **c** Representative image of perivascular fibrosis in the remote area. Scale bars, 100 μ m. **d** Myocardial interstitial fibrosis index in the non-

infarcted area (SO, $n = 5$; UT, $n = 6$; DT, $n = 7$). **e** Perivascular fibrosis index in the remote area. (SO, $n = 5$; UT, $n = 6$; DT, $n = 7$). Data are shown as box-and-whisker plots for myocardial interstitial fibrosis and perivascular fibrosis in all animals. The differences among the three groups were examined using nonparametric Kruskal–Wallis tests, followed by Dunn's tests. ** $P < 0.01$ vs. SO and † $P < 0.05$ vs. UT

In Fig. 4, a–c depict vWF staining in the hearts, vWF and SMA staining in the coronary arteries, and EVG staining in the coronary arteries, respectively, obtained in the UT and DT groups. Quantitative analysis indicated that microvessel density (the vWF staining) was more pronounced and significantly higher in the DT than in the UT group (Fig. 4d). Immunohistological analysis of the vWF-SMA revealed that the coronary artery wall was thinner (Fig. 4e), and the media-to-lumen cross-sectional area ratio was lower in the DT than in the UT group (Fig. 4f). Furthermore, the EVG staining indicated the progression of coronary artery remodeling (interstitial elastic membrane area/vascular smooth muscle area ratio [23], Fig. 4g) in the UT group compared with the DT group.

Neurohumoral and biochemical markers

Table 2 shows the plasma neurohumoral variables and biochemical parameters in post-MI SHR after 7 weeks of treatment. The plasma catecholamine, BNP, AVP, Ang II, CRP, and TNF- α levels were lower in the DT than in the UT group.

Prognosis analysis

Survival rates of 50 SHR in the SO, UT, and DT groups were examined (Fig. 5). No deaths occurred in the SO group (8/8). The survival rate of post-MI SHR during the 50-day study period was 80% (16/20) in the DT group and 41% (9/22) in the UT group ($P = 0.004$). Donepezil therapy resulted in a 66% reduction in the relative risk of death [(59–20)/59]. Regarding the cause of death, cardiac rupture was observed in neither the UT nor DT group. Among the

13 deaths in the UT group, two were classified as sudden cardiac death, and the remaining 11 as deaths from heart failure. Among the 4 deaths in the DT group, two were classified as sudden cardiac death, and the remaining two as deaths from heart failure. No statistical comparison was made on the cause of death between the UT and DT groups due to the small sample size.

Discussion

Hypertension and hypertensive hearts are the most common conditions observed in CHF [20]. The present study aimed to mimic, at least in part, such a clinical situation using a CHF model of post-MI SHR. Major findings are: chronic AChE inhibition with donepezil (1) markedly improved 50-day survival, (2) significantly reduced weekly HR and MBP, (3) prevented the progression of cardiac remodeling and dysfunction, (4) prevented the progression of coronary artery remodeling, and (5) suppressed the plasma catecholamine, BNP, AVP, Ang II, and pro-inflammatory marker levels.

The beneficial impact of donepezil on post-MI CHF associated with hypertension

This study investigated the therapeutic effects of donepezil in the treatment of CHF associated with hypertension to develop a new clinical CHF treatment strategy. Most importantly, donepezil treatment markedly improved the 50-day survival rate of post-MI SHR (Fig. 5). This result indicates that donepezil treatment, which was initiated 2 weeks after the induction of permanent MI, primarily exerts

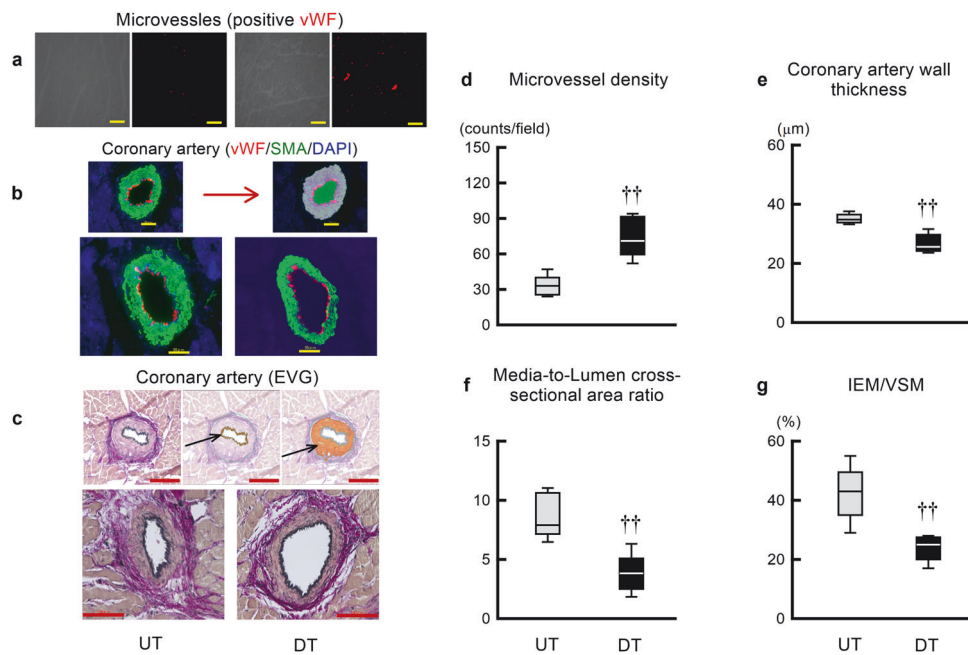


Fig. 4 Immunohistochemical, microvessel, and coronary artery analysis in the peri-infarct area of post-MI SHR in UT and DT groups. **a** Representative micrographs of von Willebrand factor (vWF, red) immunostaining. Scale bars, 100 μ m. **b** Immunofluorescent expression of coronary artery vWF (red) and smooth muscle actin SMA (green) in the non-infarcted region. Scale bars, 50 μ m. **c** Representative micrographs of coronary artery Elastic van Gison staining in the non-infarcted region (arrowheads indicate internal elastic membrane, dark brown; and vascular smooth muscle, yellow). Scale bars, 100 μ m.

d Quantitative analysis of microvessel density (UT, $n = 5$; DT, $n = 5$). **e** Quantitative analysis of coronary artery wall thickness (UT, $n = 5$; DT, $n = 5$). **f** Quantitative analysis of coronary arterial media-to-lumen cross-sectional area ratio (UT, $n = 5$; DT, $n = 5$). **g** Analysis of coronary artery internal elastic membrane (IEM) area and vascular smooth muscle (VSM) area ratio (UT, $n = 5$, DT, $n = 5$). Data are shown as box-and-whisker plots. The differences were examined by using the nonparametric Mann–Whitney U-test in two groups. $^{\dagger\dagger}P < 0.01$ vs. UT

Table 2 Plasma neurohumoral and inflammatory parameters in SO and post-MI SHR after the 7 weeks of treatment

	SO	UT	DT	<i>P</i> -value between UT and DT
Norepinephrine, pg/mL	77 \pm 8 (5)	3414 \pm 1955 (9)	183 \pm 35 (14)	0.017
Epinephrine, pg/mL	728 \pm 257 (5)	6579 \pm 2734 (9)	1121 \pm 164 (14)	< 0.001
BNP, pg/mL	392 \pm 501 (5)	757 \pm 124 (9)	349 \pm 47 (14)	0.002
AVP, pg/mL	1151 \pm 170 (5)	1479 \pm 276 (9)	897 \pm 97 (14)	0.047
Ang II, pg/mL	42 \pm 3 (5)	69 \pm 5 (9)	49 \pm 3 (14)	0.010
CRP, ng/mL	305 \pm 33 (5)	427 \pm 18 (9)	347 \pm 22 (14)	0.024
TNF- α , pg/mL	9.0 \pm 0.0 (2)	10.4 \pm 1.5(8)	5.8 \pm 1.5 (12)	0.020

BNP B-type natriuretic peptide, AVP arginine vasopressin, Ang II angiotensin II, CRP C-reactive protein, TNF- α tumor necrosis factor- α . Data are expressed as means \pm SEM (sample size). When the concentration was below the detection limit, the sample was not included in the analysis. The overall differences among the three groups were not statistically significant by Kruskal–Wallis tests. As a reference, *P*-values derived from the Mann–Whitney U-tests between UT and DT groups are shown

its beneficial effect by preventing the progression of cardiovascular remodeling and CHF-HT-related cardiac dysfunction. The improved survival outcomes highlight the potential of donepezil as a therapeutic intervention for the patient population afflicted with this condition. Donepezil is primarily used to treat AD by increasing cortical ACh levels. However, previous studies have indicated a significant association between CHF and AD, as CHF is a

common comorbidity among patients with AD [24]. Clinical studies have reported that AChE inhibition through the use of cholinesterase inhibitors such as donepezil reduces cardiovascular death and the incidence of new-onset CHF among users than among non-users [25, 26]. The complex interplay between CHF and AD is characterized by shared risk factors such as age, hypertension, and diabetes mellitus. Additionally, both conditions involve autonomic nervous

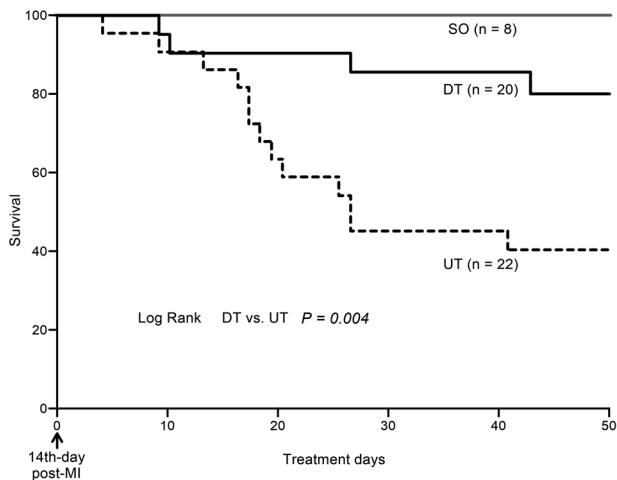


Fig. 5 Kaplan–Meier survival curves of spontaneously hypertensive rats. Kaplan–Meier survival curves of spontaneously hypertensive rats in the sham-operated group (SO, $n = 8$), those with myocardial infarction (MI) in the untreated group (UT, $n = 22$), and donepezil-treated group (DT, $n = 20$). Treatment commenced on day 14 after induction of permanent MI

system dysfunction with sympathetic activation and cholinergic neurotransmission deficiency [26].

In the present study, we demonstrated that pharmacological activation of the vagal nerve using donepezil significantly reduced the mortality rate of post-MI SHR. Based on these findings, we propose that donepezil would be a clinically viable and novel pharmacological therapy for severe CHF-HT. The positive outcomes observed in this study demonstrate the beneficial effects of donepezil on cardiovascular remodeling, cardiac function, and survival in rats with CHF-HT while offering promising prospects for its potential translation into clinical practice. However, further investigation is needed to gain a comprehensive understanding of the treatment mechanisms underlying AChE inhibition in CHF animal models and to establish an effective therapeutic strategy. For example, bradycardia, which was regarded as a beneficial effect in the present study, can be an adverse event associated with donepezil treatment [27] and needs to be cautiously monitored.

Hemodynamic and cardiovascular remodeling effects of donepezil

A telemetry system was used in this study to record BP and HR with minimum stress in conscious and freely moving rats. The results demonstrate that post-MI SHR (UT and DT groups) showed significantly higher HR and lower MBP than those of the SO rats, and treatment with donepezil reduced the weekly average HR and MBP (DT vs. UT) (Fig. 2). The bradycardic effect of donepezil may have contributed to the maintenance of cardiac function by reducing myocardial oxygen consumption, alleviating

cardiac stress, increasing coronary flow, and prolonging ventricular filling time.

Donepezil-induced HR reduction may have exerted a beneficial effect similar to that of beta-blockers, which are widely used for treating CHF [9, 28]. However, beta-blockers may not be suitable for patients with decompensated heart failure because of their potential to suppress myocardial contractility. In contrast, donepezil suppresses systemic sympathetic overactivity [16, 29], as evidenced by decreased MBP and plasma norepinephrine concentrations. Hence, the potential suppression of myocardial contractility due to sympathetic inhibition may have been partly counterbalanced by the prevention of a significant increase in systemic vascular resistance.

The mode of action of beta-blockers in the treatment of CHF is still incompletely understood [30]. The reduction of cardiac remodeling by beta-blockers is probably achieved by the inhibition of the renin-angiotensin-aldosterone system. In the present study, the DT group demonstrated significant prevention of cardiovascular remodeling and dysfunction compared with the UT group (Fig. 3 and Table 1), and notable improvements in the thinning of smooth muscle walls and reduction of media-to-lumen cross-sectional area ratio in the coronary arteries (Fig. 4). These findings indicate successful prevention of coronary artery remodeling, likely leading to reduced resistance and improved coronary perfusion. Our results conform with those of a previous study that highlighted the role of impaired parasympathetic activity in right ventricular dysfunction and pulmonary vascular remodeling in pulmonary arterial hypertension [31]. These findings further support the potential significance of our study and underscore the importance of parasympathetic modulation in cardiovascular diseases. Lower E_a and RAP values in the DT group indicate increased arterial compliance and decreased preload. These findings support previous knowledge regarding the beneficial effect of donepezil-induced HR reduction in preventing cardiac dysfunction in normotensive SD rats with chronic MI [16, 17].

SVRI was lower in the UT than in the SO group despite the significant neurohumoral activation in the UT group (Table 1), which renders the interpretation of SVRI complicated. A previous study using SD rats indicates that SVRI decreased for approximately 4 weeks after MI and returned to the control level by approximately 7 weeks [32]. Thereafter, SVRI increased with the progression of heart failure. In contrast, plasma catecholamine levels increased at 4 weeks after MI [33, 34]. These results suggest that the time course of SVRI changes after MI may not parallel with that of neurohumoral activation. Although we could not find the time course of SVRI changes in post-MI SHR in the literature, SVRI did not differ significantly between SO and post-MI SHR at approximately 4 weeks after MI [35]. We

speculate that SVRI may be regulated differently from neurohumoral activation. For instance, renal vasculature reveals local autoregulation of renal blood flow even in the ex-vivo kidney [36], indicating that renal vascular resistance, which should affect SVRI, can be changed independently of neurohumoral status. No significant difference in SVRI between the UT and DT groups also suggests the disparity between SVRI and neurohumoral activation.

Neurohumoral and inflammatory effects of donepezil

Donepezil administration suppresses AChE activity, resulting in increased central and peripheral ACh levels. This, in turn, exerts bradycardic and antihypertensive effects by decreasing sympathetic outflow, increasing parasympathetic tone, or both. Additionally, angiogenesis is significantly promoted. The $\alpha 7$ -nicotinic ACh receptor ($\alpha 7$ -nAChR) is widely distributed in peripheral neural and non-neural tissues and plays a role in cholinergic anti-inflammatory response [37]. The vagal afferent fibers transmit inflammatory signals to the central nervous system, resulting in increased vagal efferent output. This modulation of inflammation, immunity, and angiogenesis via peripheral $\alpha 7$ -nAChR [38, 39] may have contributed to the angiogenic effects observed following donepezil treatment [19].

The DT group showed significantly reduced plasma catecholamine and AVP levels, consistent with the findings of our previous studies on normotensive rats with CHF [16]. Additionally, the DT group exhibited significantly lower plasma Ang II and BNP levels than those of the UT group (Table 2), which may be attributed to donepezil-induced augmented vagal tone and diminished sympathetic outflow. This improved neurohormonal profile further supports the cardioprotective effects of donepezil.

Study limitations

First, we used post-MI SHR as the CHF-HT model to mimic the clinical condition of patients. However, because MI was artificially induced, the extent to which this model mimics the clinical CHF-HT parameters remains unknown. Moreover, patients with CHF-HT often receive diverse pharmacological treatments; hence, assessing the efficacy of a single drug treatment is challenging.

Secondly, the present study design did not allow us to determine whether sympathetic suppression observed in the DT group compared with the UT group was the direct effect of donepezil or the indirect effect resulting from the improvement of CHF. The MBP under conscious state was lower in the DT than in the UT group from week 1 of treatment (Fig. 2b), suggesting that sympathetic suppression

preceded the significant improvement in CHF conditions. In contrast, lower plasma catecholamine levels in the DT than in the UT group after 7 weeks of treatment (Table 2) probably reflected both the direct sympathoinhibitory effect and the indirect effect through the improvement of CHF. To answer this question, further studies are required such as that elucidates the time course of plasma catecholamine levels following the treatment with donepezil.

Finally, we observed higher MBP levels in the UT than in the DT group during conscious hemodynamic monitoring (Fig. 2). In contrast, MBP was lower in the UT than in the DT group when the rats were under anesthesia (Table 1). These findings suggest that conscious animals in the UT group may exhibit sympathetic overactivity relative to those in the DT group, and inducing anesthesia may have partly mitigated the sympathetic effect and reversed the MBP levels between the UT and DT groups. This interpretation is supported by the improved systolic function in the DT group compared with the UT group under anesthesia. Unfortunately, we were unable to draw pressure-volume loops for a more comprehensive examination of cardiac function due to the lack of absolute LV volume data. Ideally, the LV volume data should have been obtained using echocardiography or other modalities.

In conclusion, this study demonstrates that inhibition of AChE with donepezil is a highly effective approach for preventing cardiovascular remodeling and improving survival in rats with severe CHF-HT. Donepezil promises a therapeutic option for patients with this challenging condition. However, further studies are required to evaluate the efficacy and safety of this therapy for clinical application.

Data availability

The datasets used and/or analyzed in the current study are available from the corresponding author upon reasonable request.

Author contributions Meihua Li and Can Zheng designed and performed the experiments. Meihua Li performed the statistical analyses and drafted the first manuscript. Toru Kawada, Kazunori Uemura, Shohei Yokota, Hiroki Matsushita, and Keita Saku interpreted the results. Toru Kawada and Keita Saku edited and reviewed the manuscript. All authors commented on the previous versions of the manuscript and read and approved the final manuscript.

Funding This study was partly supported by JSPS KAKENHI (grant numbers 26461099, 26430103, 20K20622, 22K08222), the research program of the Japan Agency for Medical Research and Development (22ama121050j0001), the Research Program of the Ministry of Internal Affairs and Communications (SCOPE: JP225006004), the Intramural Research Fund for Cardiovascular Diseases of the National Cerebral and Cardiovascular Center (21-2-7, 21-2-9), a research grant from JST (JPMJPF2018), and the research grant from NTT Research, Inc. The authors confirm that the funders did not influence the study design, contents of the article, or selection of this journal.

Compliance with ethical standards

Ethics approval and consent to participate Animal care protocols and all experiments were performed in strict accordance with the Guiding Principles for the Care and Use of Animals in the Field of Physiological Science, which was approved by the Physiological Society of Japan. All protocols were reviewed and approved by the Animal Subject Committee of the National Cerebral and Cardiovascular Center (#15004 and #16002).

Conflict of interest The authors declare no competing interests.

Research involving human participants and/or animals This study did not involve human participants. The Animal Subject Committee of the National Cerebral and Cardiovascular Center has approved the animal experiments.

References

1. Yancy CW, Jessup M, Bozkurt B, Butler J, Casey DE, Jr Colvin MM, et al. 2017 ACC/AHA/HFSA Focused Update of the 2013 ACCF/AHA Guideline for the Management of Heart Failure: A report of the American college of cardiology/american heart association task force on clinical practice guidelines and the heart failure society of America. *J Card Fail.* 2017. <https://doi.org/10.1016/j.cardfail.2017.04.014>.
2. Ponikowski P, Voors AA, Anker SD, Bueno H, Cleland JG, Coats AJ, et al. 2016 ESC Guidelines for the diagnosis and treatment of acute and chronic heart failure: The Task Force for the diagnosis and treatment of acute and chronic heart failure of the European Society of Cardiology (ESC). Developed with the special contribution of the Heart Failure Association (HFA) of the ESC. *Eur J Heart Fail.* 2016;18:891–975.
3. Oparil S, Schmieder RE. New approaches in the treatment of hypertension. *Circ Res.* 2015;116:1074–95.
4. Androne AS, Hryniewicz K, Goldsmith R, Arwady A, Katz SD. Acetylcholinesterase inhibition with pyridostigmine improves heart rate recovery after maximal exercise in patients with chronic heart failure. *Heart.* 2003;89:854–8.
5. La Rovere MT, Bigger JT Jr, Marcus FI, Mortara A, Schwartz PJ. Baroreflex sensitivity and heart-rate variability in prediction of total cardiac mortality after myocardial infarction. ATRAMI (Autonomic Tone and Reflexes After Myocardial Infarction) Investigators. *Lancet.* 1998;351:478–84.
6. Packer M. The neurohormonal hypothesis: a theory to explain the mechanism of disease progression in heart failure. *J Am Coll Cardiol.* 1992;20:248–54.
7. Rosenwinkel ET, Bloomfield DM, Arwady MA, Goldsmith RL. Exercise and autonomic function in health and cardiovascular disease. *Cardiol Clin.* 2001;19:369–87.
8. Binkley PF, Nunziata E, Haas GJ, Nelson SD, Cody RJ. Parasympathetic withdrawal is an integral component of autonomic imbalance in congestive heart failure: demonstration in human subjects and verification in a paced canine model of ventricular failure. *J Am Coll Cardiol.* 1991;18:464–72.
9. McDonagh TA, Metra M, Adamo M, Gardner RS, Baumbach A, Bohm M, et al. 2021 ESC Guidelines for the diagnosis and treatment of acute and chronic heart failure. *Eur Heart J.* 2021;42:3599–726.
10. Kleiger RE, Miller JP, Bigger JT Jr, Moss AJ. Decreased heart rate variability and its association with increased mortality after acute myocardial infarction. *Am J Cardiol.* 1987;59:256–62.
11. Odemuyiwa O, Malik M, Farrell T, Bashir Y, Poloniecki J, Camm J. Comparison of the predictive characteristics of heart rate variability index and left ventricular ejection fraction for all-cause mortality, arrhythmic events and sudden death after acute myocardial infarction. *Am J Cardiol.* 1991;68:434–9.
12. Li M, Zheng C, Sato T, Kawada T, Sugimachi M, Sunagawa K. Vagal nerve stimulation markedly improves long-term survival after chronic heart failure in rats. *Circulation.* 2004;109:120–4.
13. De Ferrari GM, Crijns HJ, Borggrefe M, Milasinovic G, Smid J, Zabel M, et al. Chronic vagus nerve stimulation: a new and promising therapeutic approach for chronic heart failure. *Eur Heart J.* 2011;32:847–55.
14. Premchand RK, Sharma K, Mittal S, Monteiro R, Dixit S, Libbus I, et al. Autonomic regulation therapy via left or right cervical vagus nerve stimulation in patients with chronic heart failure: results of the ANTHEM-HF trial. *J Card Fail.* 2014;20:808–16.
15. Gold MR, Van Veldhuisen DJ, Hauptman PJ, Borggrefe M, Kubo SH, Lieberman RA, et al. Vagus nerve stimulation for the treatment of heart failure: the INOVATE-HF trial. *J Am Coll Cardiol.* 2016;68:149–58.
16. Li M, Zheng C, Kawada T, Inagaki M, Uemura K, Shishido T, et al. Donepezil markedly improves long-term survival in rats with chronic heart failure after extensive myocardial infarction. *Circ J.* 2013;77:2519–25.
17. Li M, Zheng C, Kawada T, Inagaki M, Uemura K, Sugimachi M. Adding the acetylcholinesterase inhibitor, donepezil, to losartan treatment markedly improves long-term survival in rats with chronic heart failure. *Eur J Heart Fail.* 2014;16:1056–65.
18. Li M, Zheng C, Kawada T, Inagaki M, Uemura K, Sugimachi M. Intracerebroventricular infusion of donepezil prevents cardiac remodeling and improves the prognosis of chronic heart failure rats. *J Physiol Sci.* 2020;70:11.
19. Li M, Zheng C, Kawada T, Inagaki M, Uemura K, Akiyama T, et al. Impact of peripheral $\alpha 7$ -nicotinic acetylcholine receptors on cardioprotective effects of donepezil in chronic heart failure rats. *Cardiovasc Drugs Ther.* 2021;35:877–88.
20. Shimokawa H, Miura M, Nochioka K, Sakata Y. Heart failure as a general pandemic in Asia. *Eur J Heart Fail.* 2015;17:884–92.
21. Humphrey JD. Mechanisms of vascular remodeling in hypertension. *Am J Hypertens.* 2021;34:432–41.
22. Itter G, Jung W, Juretschke P, Schoelkens BA, Linz W. A model of chronic heart failure in spontaneous hypertensive rats (SHR). *Lab Anim.* 2004;38:138–48.
23. Brown IAM, Diederich L, Good ME, DeLalio LJ, Murphy SA, Cortese-Krott MM, et al. Vascular smooth muscle remodeling in conductive and resistance arteries in hypertension. *Arterioscler Thromb Vasc Biol.* 2018;38:1969–85.
24. Avitan I, Halperin Y, Saha T, Bloch N, Atrahimovich D, Polis B, et al. Towards a consensus on Alzheimer's disease comorbidity? *J Clin Med.* 2021;10:4360.
25. Nordstrom P, Religa D, Wimo A, Winblad B, Eriksdotter M. The use of cholinesterase inhibitors and the risk of myocardial infarction and death: a nationwide cohort study in subjects with Alzheimer's disease. *Eur Heart J.* 2013;34:2585–91.
26. Hsieh MJ, Chen DY, Lee CH, Wu CL, Chen YJ, Huang YT, et al. Association between cholinesterase inhibitors and new-onset heart failure in patients with Alzheimer's disease: a nationwide propensity score matching study. *Front Cardiovasc Med.* 2022;9:831730.
27. Morris R, Luboff H, Jose RP, Eckhoff K, Bu K, Pham M, et al. Bradycardia due to donepezil in adults: systematic analysis of FDA adverse event reporting system. *J Alzheimers Dis.* 2021;81:297–307.
28. Baumgartner H, Falk V, Bax JJ, De Bonis M, Hamm C, Holm PJ, et al. 2017 ESC/EACTS Guidelines for the management of valvular heart disease. *Eur Heart J.* 2017;38:2739–91.
29. Li M, Zheng C, Kawada T, Uemura K, Inagaki M, Saku K, et al. Early donepezil monotherapy or combination with metoprolol

- significantly prevents subsequent chronic heart failure in rats with reperfused myocardial infarction. *J Physiol Sci.* 2022;72:12.
30. Silke B. Beta-blockade in CHF: pathophysiological considerations. *Eur Heart J.* 2006;8:C13–8.
 31. da Silva Goncalves Bos D, Van Der Bruggen CEE, Kurakula K, Sun XQ, Casali KR, Casali AG, et al. Contribution of impaired parasympathetic activity to right ventricular dysfunction and pulmonary vascular remodeling in pulmonary arterial hypertension. *Circulation.* 2018;137:910–24.
 32. DeFelice A, Frering R, Horan P. Time course of hemodynamic changes in rats with healed severe myocardial infarction. *Am J Physiol.* 1989;257:H289–96.
 33. Collister JP, Hartnett C, Mayerhofer T, Nahey D, Stauthammer C, Krüger M, et al. Overexpression of copper/zinc superoxide dismutase in the median preoptic nucleus improves cardiac function after myocardial infarction in the rat. *Clin Exp Pharm Physiol.* 2016;43:960–6.
 34. Miao Y, Li M, Wang C, Li H, Chen H. Effect of β -adrenergic receptor kinase inhibitor on post-myocardial infarction heart failure in rats. *Int J Clin Exp Pathol.* 2017;10:9858–65.
 35. Fletcher PJ, Pfeffer JM, Pfeffer MA. Altered sensitivity to increases in vascular resistance in rats with hypertension and myocardial infarction. *Am Heart J.* 1986;111:120.
 36. Cupples WA, Braam B. Assessment of renal autoregulation. *Am J Physiol Ren Physiol.* 2007;292:F1105–23.
 37. Andersson U, Tracey KJ. Neural reflexes in inflammation and immunity. *J Exp Med.* 2012;209:1057–68.
 38. Wang H, Yu M, Ochani M, Amella CA, Tanovic M, Susarla S, et al. Nicotinic acetylcholine receptor $\alpha 7$ subunit is an essential regulator of inflammation. *Nature.* 2003;421:384–8.
 39. Hashimoto T, Ichiki T, Watanabe A, Hurt-Camejo E, Michaelsson E, Ikeda J, et al. Stimulation of $\alpha 7$ nicotinic acetylcholine receptor by AR-R17779 suppresses atherosclerosis and aortic aneurysm formation in apolipoprotein E-deficient mice. *Vasc Pharm.* 2014;61:49–55.

Publisher's note Springer Nature remains neutral with regard to jurisdictional claims in published maps and institutional affiliations.

Springer Nature or its licensor (e.g. a society or other partner) holds exclusive rights to this article under a publishing agreement with the author(s) or other rightsholder(s); author self-archiving of the accepted manuscript version of this article is solely governed by the terms of such publishing agreement and applicable law.